Dynamics of the fluid balancer (Diversity and Universality of Nonlinear Wave Phenomena)

AUTHOR(S):

Langthjem, Mikael A.; Nakamura, Tomomichi

CITATION:

Langthjem, Mikael A. ...[et al]. Dynamics of the fluid balancer (Diversity and Universality of Nonlinear Wave Phenomena). 数理解析研究所講究録 2011, 1761: 140-150

ISSUE DATE:

2011-09

URL:

http://hdl.handle.net/2433/171353

数理解析研究所講究録
第1761巻 2011年 140-150

Dynamics of the fluid balancer

Mikael A. Langthjem†, Tomomichi Nakamura‡

†Faculty of Engineering, Yamagata University,
Jonan 4-chome, Yonezawa, 992-8510 Japan

‡Department of Mechanical Engineering, Osaka Sangyo University,
3-1-1 Nakagaito, Daito-shi, Osaka, 574-853001 Japan

Abstract

The paper is concerned with the dynamics of a so-called fluid balancer; a hula hoop ring-like structure containing a small amount of liquid which, during rotation, is spun out to form a thin liquid layer on the inner surface of the ring. The liquid is able to counteract unbalance mass in an elastically mounted rotor. The paper derives the equations of motion for the coupled fluid-structure system, with the fluid equations based on shallow water theory. An analytical solution to a simplified version of the shallow water equations, describing a hydraulic jump, is discussed in detail.

1 Introduction

A fluid balancer is used on rotating machinery to eliminate the undesirable effects of unbalance mass. It has become a standard feature on most household washing machines, but is also used on heavy industrial rotating machinery. Taking the washing machine fluid balancer as example, it consists of a hollow ring, like a hula hoop ring but typically with rectangular cross sections, which contains a small amount of liquid. When the ring is rotating at a high angular velocity Ω the liquid will form a thin liquid layer on the inner surface of the outermost wall, as sketched in Fig. 1. Consider the situation where an unbalance mass m is present; for example the clothes in a washing machine. The rotor has a critical angular velocity Ω_{cr} where the centripetal forces are in balance with the forces due to the restoring springs. Below this velocity ($\Omega < \Omega_{cr}$) the mass center of the fluid will be located 'on the same side' as the unbalance mass, as shown in the left part of Fig. 1. [Here M indicates the mass of the empty rotor and $\mathcal{M}$ the mass of the contained liquid.] At a certain supercritical angular velocity ($\Omega > \Omega_{cr}$) the mass center of the liquid will move to the 'opposite side' of the unbalance mass, as shown in the right part of Fig. 1, resulting in 'mass balance' and thus in a reduced oscillation amplitude of the rotor.

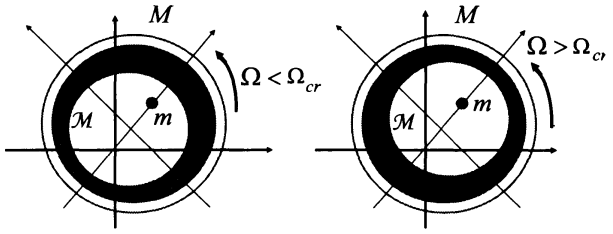

Figure 1: Working principle of the fluid balancer.

This is the working principle of the fluid balancer, which has been verified experimentally [1]; but no conclusive explanation has been given so far. It is the aim of the present project to attempt giving an analytical explanation.

The present work builds upon a large number of studies into the dynamics and stability of rotors partially filled with liquid [2, 3]. Non-linear studies have been carried out by Berman *et al.* [4], Colding-Jorgensen [5], Kasahara *et al.* [6], and Yoshizumi [7]. Berman *et al.* [4] found, both by numerical analysis and by experiment, that non-linear surfaces can exist in the form of hydraulic jumps, undular bores, and solitary waves. [An undular bore is a relatively weak hydraulic jump, with undulations behind it.] Colding-Jorgensen [5] studied solely a hydraulic jump solution, in the spirit of the analysis of [4] . On the contrary to [4] and [5] the studies of Kasahara *et al.* [6] and Yoshizumi [7] are purely numerical.

To the best of our knowledge, the effect of an unbalance mass has not been studied before. The system (with an unbalance mass) is however closely related to the so-called automatic dynamic balancer [8] where a number of balls running in a circular groove play the sam role as the liquid layer in the present study.

As [5] the present study is based largely on the approach of Berman *et al.* [4]. However, contrary to the one-degree-of-freedom assumption in [4, 5], the present work considers a rotor with two degrees of freedom.

2 Rotor equation

Consider a rotating vessel (rotating fluid chamber) of mass M equipped with a small unbalance mass m located a distance s from the geometric center, and containing a small amount of liquid, as sketched in Fig. 2. The inner radius of the vessel is R. The rotor is supported by springs, with spring constant K, in the $\bar{X}$ and $\bar{Y}$ directions. The structural damping forces in these directions are proportional to the parameter C. Let the coordinate system $(\bar{x}, \bar{y})$ rotate with the constant angular velocity Ω about the fixed system $(\bar{X}, \bar{Y})$.

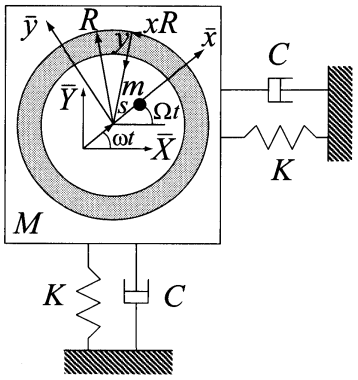

Figure 2: Definition of coordinate systems and some of the symbols used.

In terms of the fixed coordinate system the equation of motion of the rotor is given by

$$\begin{bmatrix} M+m & 0 \\ 0 & M+m \end{bmatrix} \begin{Bmatrix} \ddot{X}_r \\ \ddot{Y}_r \end{Bmatrix} + \begin{bmatrix} C & 0 \\ 0 & C \end{bmatrix} \begin{Bmatrix} \dot{X}_r \\ \dot{Y}_r \end{Bmatrix} + \begin{bmatrix} K_x & 0 \\ 0 & K_y \end{bmatrix} \begin{Bmatrix} X_r \\ Y_r \end{Bmatrix} = ms\Omega^2 \begin{Bmatrix} \cos\Omega t \\ \sin\Omega t \end{Bmatrix} + \begin{Bmatrix} F_X \\ F_Y \end{Bmatrix}. \tag{1}$$

Here X_r and Y_r are the deflections of the rotor and F_Y, F_Y are the fluid force components acting thereon. An 'overdot' denotes differentiation with respect to time t. The first term on the right hand side shows that, in a fixed coordinate system, the unbalance mass introduces a periodic forcing.

It will, however, be more convenient to consider the coupled fluid-rotor motion in terms of the rotating coordinate system $(\bar{x}, \bar{y})$. The deflections in the two coordinate systems are related by the transformations

$$\left\{ \begin{array}{c} x_r \\ y_r \end{array} \right\} = \left[\begin{array}{cc} \cos\Omega t & \sin\Omega t \\ -\sin\Omega t & \cos\Omega t \end{array} \right] \left\{ \begin{array}{c} X_r \\ Y_r \end{array} \right\}, \quad \left\{ \begin{array}{c} X_r \\ Y_r \end{array} \right\} = \left[\begin{array}{cc} \cos\Omega t & -\sin\Omega t \\ \sin\Omega t & \cos\Omega t \end{array} \right] \left\{ \begin{array}{c} x_r \\ y_r \end{array} \right\}. \tag{2}$$

Applying (2) to (1) we obtain the equation of motion in terms of rotating coordinates as

$$\begin{aligned} &\left[\begin{array}{cc} M+m & 0 \\ 0 & M+m \end{array} \right] \left\{ \begin{array}{c} \ddot{x}_r \\ \ddot{y}_r \end{array} \right\} + \left[\begin{array}{cc} C & -2(M+m)\Omega \\ 2(M+m)\Omega & C \end{array} \right] \left\{ \begin{array}{c} \dot{x}_r \\ \dot{y}_r \end{array} \right\} \\ + &\left[\begin{array}{cc} K_x - (M+m)\Omega^2 & -C\Omega \\ C\Omega & K_y - (M+m)\Omega^2 \end{array} \right] \left\{ \begin{array}{c} x_r \\ y_r \end{array} \right\} \\ = &\left\{ \begin{array}{c} ms\Omega^2 \\ 0 \end{array} \right\} + \left\{ \begin{array}{c} F_x \\ F_y \end{array} \right\}. \end{aligned} \tag{3}$$

It is seen that, in this coordinate system, the unbalance mass introduces a force, proportional to Ω^2, acting in the $\bar{x}$-direction.

In order to evaluate the body force acting on the fluid, the acceleration vector expressed in the rotating coordinate system will be needed; it is given by

$$\left\{ \begin{array}{c} \ddot{\mathfrak{X}}_r \\ \ddot{\mathfrak{Y}}_r \end{array} \right\} = \left[\begin{array}{cc} 1 & 0 \\ 0 & 1 \end{array} \right] \left\{ \begin{array}{c} \ddot{x}_r \\ \ddot{y}_r \end{array} \right\} + 2\Omega \left[\begin{array}{cc} 0 & -1 \\ 1 & 0 \end{array} \right] \left\{ \begin{array}{c} \dot{x}_r \\ \dot{y}_r \end{array} \right\} - \Omega^2 \left[\begin{array}{cc} 1 & 0 \\ 0 & 1 \end{array} \right] \left\{ \begin{array}{c} x_r \\ y_r \end{array} \right\}. \tag{4}$$

3 Fluid equations

3.1 The shallow water equations

The fluid motion in the rotating vessel will be described by a shallow water approximation of the Navier-Stokes equations, and in terms of a coordinate system (x, y) attached to the wall of the rotor, as shown in Fig. 2. This coordinate system is related to a polar coordinate system (r, θ) attached to the rotor (such that $\bar{x} = r\cos\theta$, $\bar{y} = r\sin\theta$) in the following way:

$$x = R\theta, \quad y = R - r, \tag{5}$$

where R is the radius of the vessel; see again Fig. 2. x, y are rectangular (Cartesian) coordinates, indicating that curvature effects will be ignored. This is permissable when the fluid layer thickness $h(t, x)$ is sufficiently small in comparison with the vessel radius R, i.e., $|h(t,x)|/R \ll 1$ for all x, t.

Under these assumptions the fluid equations of motion can be written as [4, 9]

$$\frac{\partial u}{\partial t} + u\frac{\partial u}{\partial x} + v\frac{\partial u}{\partial y} - 2\Omega v = -\frac{1}{\rho}\frac{\partial p}{\partial x} + \nu\frac{\partial^2 u}{\partial y^2} + \ddot{\mathfrak{X}}_r \sin(x/R) - \ddot{\mathfrak{Y}}_r \cos(x/R), \tag{6}$$

$$\frac{\partial v}{\partial t} + 2\Omega u + R\Omega^2 = -\frac{1}{\rho}\frac{\partial p}{\partial y}. \tag{7}$$

Here u and v are the fluid velocity components in the x and y directions, p is the fluid pressure, ρ is the fluid density, and ν the kinematic viscosity of the fluid.

The continuity equation is

$$\frac{\partial u}{\partial x} + \frac{\partial v}{\partial y} = 0. \tag{8}$$

The boundary conditions are

$$u(0) = 0, \quad v(0) = 0, \tag{9}$$
$$\left(\frac{\partial h}{\partial t} + u\frac{\partial h}{\partial x}\right)_{y=h} = v(h), \quad p(h) = 0,$$

where, again, $h(t, x)$ specifies the free surface of the fluid layer.

In the shallow water approximation it is assumed that

$$v(t, x, y) = \frac{y}{h_0}\frac{\partial h}{\partial t}, \tag{10}$$

where h_0 is the mean fluid depth. Then (7) can be written as

$$\frac{y}{h_0}\frac{\partial^2 h}{\partial t^2} + 2\Omega u + R\Omega^2 = -\frac{1}{\rho}\frac{\partial p}{\partial y}. \tag{11}$$

This equation can be integrated, to give

$$\frac{1}{\rho}p(y) = \frac{1}{2h_0}\left(h_0^2 - y^2\right)\frac{\partial^2 h}{\partial t^2} + 2\Omega\int_y^h u\, dy + R\Omega^2(h - y). \tag{12}$$

Inserting (12) into (6) we get

$$\frac{\partial u}{\partial t} + u\frac{\partial u}{\partial x} + v\frac{\partial u}{\partial y} = -R\Omega^2\frac{\partial h}{\partial x} + 2\Omega\frac{\partial h}{\partial t} - \frac{1}{2h_0}(h_0^2 - y^2)\frac{\partial^3 h}{\partial x \partial t^2} + \nu\frac{\partial^2 u}{\partial y^2} + \mathfrak{F}, \tag{13}$$

where, here and in the following,

$$\mathfrak{F} = \ddot{\mathfrak{X}}_r \sin(x/R) - \ddot{\mathfrak{Y}}_r \cos(x/R). \tag{14}$$

Let

$$U = \frac{1}{h}\int_0^h u\, dy \tag{15}$$

denote the mean flow velocity in the x-direction. Applying this 'operator' to (13) we get

$$\frac{\partial U}{\partial t} + U\frac{\partial U}{\partial x} + \frac{h_0}{3}\frac{\partial^3 h}{\partial x \partial t^2} + R\Omega^2\frac{\partial h}{\partial x} - 2\Omega\frac{\partial h}{\partial t} - \eta U^2 - \nu_{ev}\frac{\partial^2 U}{\partial x^2} = \mathfrak{F}, \tag{16}$$

where

$$\eta U^2 \doteq -\frac{\nu}{h_0}\left[\frac{\partial u}{\partial y}\right]_{y=0}, \tag{17}$$
$$\nu_{ev}\frac{\partial^2 U}{\partial x^2} \doteq -\frac{\partial}{\partial x}\frac{1}{h_0}\int_0^{h_0}(u - U)^2 dy$$

are models for dissipation due to wall friction and internal fluid friction, respectively [4, 9]. In the first equation η is a friction coefficient (known from head loss in pipe flow) and ν_{ev} in the second equation is a so-called eddy viscosity coefficient. In (16) and (17) it has been used that

$$\frac{1}{h}\int_0^h u\frac{\partial u}{\partial x}\, dy + \frac{1}{h}\int_0^h v\frac{\partial u}{\partial y}\, dy \approx \tag{18}$$
$$\frac{\partial}{\partial x}\frac{1}{h_0}\int_0^{h_0}(u - U)^2\, dy + \underbrace{\frac{1}{h_0}U\int_0^{h_0}\frac{\partial u}{\partial x}\, dy}_{U\frac{\partial U}{\partial x}}.$$

Applying (15) to the continuity equation (8), the latter can be written as

$$\frac{\partial h}{\partial t} = -\frac{\partial (hU)}{\partial x}. \tag{19}$$

At this point we introduce the 'traveling wave' variable

$$\xi = x/R + (\Omega - \omega)t \tag{20}$$

Here ω is the angular whirling velocity of the vessel, which is assumed to be close, but not equal, to the imposed angular velocity Ω. Writing

$$U = U(\xi), \quad h = h_0 + h'(\xi), \tag{21}$$

(16) can be written as

$$\begin{aligned} &-\Omega(\Omega - 2\omega)\frac{\partial h'}{\partial \xi} + (\Omega - \omega)\frac{\partial U}{\partial \xi} = \\ &-\frac{U}{R}\frac{\partial U}{\partial \xi} + \frac{\nu_T}{R^2}\frac{\partial^2 U}{\partial \xi^2} + \eta U^2 - \frac{h_0}{3}\frac{(\Omega - \omega)^2}{R}\frac{\partial^3 h'}{\partial \xi^3} + \ddot{\mathfrak{X}}_r \sin(x/R) - \ddot{\mathfrak{Y}}_r \cos(x/R) \end{aligned} \tag{22}$$

The continuity equation (19) can be written as

$$(\Omega - \omega)\frac{\partial h'}{\partial \xi} + \frac{h_0}{R}\frac{\partial U}{\partial \xi} = -\frac{U}{R}\frac{\partial h'}{\partial \xi} - \frac{1}{R}h'\frac{\partial U}{\partial \xi}. \tag{23}$$

It is noted that the left sides of (22) and (23) are linear in the unknown variables U and h', while the right sides are non-linear. In the following we consider the linearized equations. In order for them to have a non-trivial solution, the determinant must be equal to zero,

$$\begin{vmatrix} -\Omega(\Omega - 2\omega) & \Omega - \omega \\ \Omega - \omega & h_0/R \end{vmatrix} = 0. \tag{24}$$

The possible whirling frequencies are thus

$$\omega = \Omega\left[1 + \frac{h_0}{R} \pm \left\{\frac{h_0}{R}\left(1 + \frac{h_0}{R}\right)\right\}^{\frac{1}{2}}\right]. \tag{25}$$

As the speed of the cylinder is $R\Omega$, the possible speeds of a traveling surface wave are

$$c_\pm = R\Omega\left[\frac{h_0}{R} \pm \left\{\frac{h_0}{R}\left(1 + \frac{h_0}{R}\right)\right\}^{\frac{1}{2}}\right]. \tag{26}$$

3.2 Non-dimensionalization

In order to recast the governing fluid differential equations into non-dimensional form the following parameters are introduced:

$$\begin{aligned} &\epsilon = \frac{\frac{1}{2}\rho R^2 L}{M}, \quad \delta = \frac{h_0}{R}, \quad \kappa = \frac{h'}{R}, \quad \omega_* = \frac{\omega}{\omega_s}, \quad \omega_s = \sqrt{\frac{K}{M}}, \quad \Omega_* = \frac{\Omega}{\omega_s}, \\ &t_* = \epsilon\Omega\sqrt{\frac{h_0}{R}}t, \quad c_0 = R\Omega\sqrt{\frac{h_0}{R}}, \quad x_* = \frac{x_r}{h_0}, \quad y_* = \frac{y_r}{h_0}, \\ &p_* = \frac{p}{\frac{1}{2}\rho c_0^2}, \quad \epsilon U_* = \frac{U}{c_0}, \quad \eta_* = R\eta, \quad \nu_* = \nu_{ev}\frac{M}{KR^2}. \end{aligned} \tag{27}$$

The parameter c_0 corresponds to the shallow water wave speed $(gh_0)^{\frac{1}{2}}$, but here the gravity acceleration g is the centrifugal acceleration $R\Omega^2$.

The parameter ϵ expresses, except for a factor 2π, the ratio between fluid mass and the mass of the (empty) rotor. It is assumed to be small and is used in (27) and the following as a 'bookkeeping parameter', in order to compare the magnitude of the individual terms.

A non-dimensional version of (22) can now be obtained as follows

$$\begin{aligned} &-(1-2\tilde{\omega})\frac{\partial \kappa}{\partial \xi}+\delta^{-\frac{1}{2}}(1-\tilde{\omega})\frac{\partial U_*}{\partial \xi}= \\ &-\epsilon U_*\frac{\partial U_*}{\partial \xi}+\epsilon\nu_*\frac{\partial^2 U_*}{\partial \xi^2}+\epsilon\eta_* U_*^2-\epsilon\frac{1}{3}\delta(1-\tilde{\omega})^2\left(\frac{1}{\epsilon}\frac{\partial^3\kappa}{\partial\xi^3}\right) \\ &+\epsilon\left[\epsilon^2\delta x_*''-2\epsilon\delta^{\frac{1}{2}}y_*'-x_*\right]\sin\frac{x}{R}-\epsilon\left[\epsilon^2\delta y_*''+2\epsilon\delta^{\frac{1}{2}}x_*'-y_*\right]\cos\frac{x}{R} \end{aligned} \tag{28}$$

where $\tilde{\omega}=\omega/\Omega=\omega_*/\Omega_*$. A dash refers to differentiation with respect to t_*.

The continuity equation (23) can be written as

$$(1-\tilde{\omega})\delta^{-\frac{1}{2}}\frac{\partial \kappa}{\partial \xi}+\frac{\partial U_*}{\partial \xi}=-\epsilon\left\{U_*\frac{\partial \kappa}{\partial \xi}+\kappa\frac{\partial U_*}{\partial \xi}\right\} \tag{29}$$

3.3 Perturbation analyis

The variables which are functions of the 'traveling wave parameter' ξ are expanded as follows:

$$\kappa=\kappa_0+\epsilon\kappa_1+\cdots,\quad U_*=U_0+\epsilon U_1+\cdots,\quad \tilde{\omega}=\tilde{\omega}_0+\epsilon\tilde{\omega}_1+\cdots. \tag{30}$$

Collecting the coefficients of ϵ^0 we obtain the non-dimensional versions of the left hand sides of (22) and (23),

$$-(1-2\tilde{\omega}_0)\frac{\partial \kappa_0}{\partial \xi}+\delta^{-\frac{1}{2}}(1-\tilde{\omega}_0)\frac{\partial U_0}{\partial \xi}=0, \tag{31}$$

$$\delta^{-\frac{1}{2}}(1-\tilde{\omega}_0)\frac{\partial \kappa_0}{\partial \xi}+\frac{\partial U_0}{\partial \xi}=0. \tag{32}$$

The determinant equation,

$$\begin{vmatrix} -(1-2\tilde{\omega}_0) & \delta^{-\frac{1}{2}}(1-\tilde{\omega}_0) \\ \delta^{-\frac{1}{2}}(1-\tilde{\omega}_0) & 1 \end{vmatrix}=0, \tag{33}$$

then gives the non-dimensional version of (25),

$$\tilde{\omega}_0=1+\delta\pm(\delta+\delta^2)^{\frac{1}{2}}. \tag{34}$$

The non-dimensional version of the wave number equation (26) is

$$c_\pm=c_0\left\{\delta^{\frac{1}{2}}\pm(1+\delta)^{\frac{1}{2}}\right\}, \tag{35}$$

In (35) the + solution corresponds to progressive waves and the − solution to a retrograde wave. Experiments show that only the latter type exists; accordingly the − solution is used in the following. The continuity equation (32) now gives

$$U_0=\frac{c_-}{c_0}\kappa_0=\left\{\delta^{\frac{1}{2}}-(1+\delta)^{\frac{1}{2}}\right\}\frac{\partial \kappa_0}{\partial \xi}. \tag{36}$$

Employing this expression, the terms proportional to ϵ^1 in the expansion of (28) can be written as

$$A_1\frac{\partial\kappa_0}{\partial\xi} - B_1\kappa_0\frac{\partial\kappa_0}{\partial\xi} - C_1\frac{\partial^3\kappa_0}{\partial\xi^3} + D_1\frac{\partial^2\kappa_0}{\partial\xi^2} + E_1\kappa_0^2 = x_*\sin\xi - y_*\cos\xi, \tag{37}$$

where

$$A_1 = -2\tilde{\omega}_1\frac{\sqrt{\delta+\delta^2}}{\delta}, \quad B_1 = 3\left(\frac{c_-}{c_0}\right)^2, \quad C_1 = \frac{1}{3\epsilon}\delta^2\left(\frac{c_-}{c_0}\right)^2, \tag{38}$$
$$D_1 = \nu_*\frac{c_-}{c_0}, \quad E_1 = \eta_*\left(\frac{c_-}{c_0}\right)^2.$$

In (37) it has been assumed that $\sin\xi \approx \sin x/R$ and $\cos\xi \approx \cos x/R$.

The non-dimensional version of the pressure equation (12), evaluated on the vessel surface $y = 0$, takes the form

$$p_*(0) = \epsilon\left\{\delta^2\left(\frac{c_-}{c_0}\right)^2\frac{\partial^2\kappa_0}{\partial\xi^2} + 2\left(1 + 2\delta^{\frac{1}{2}}\frac{c_-}{c_0}\right)\kappa_0\right\} + O(\epsilon^2). \tag{39}$$

4 Fluid-structure coupling

4.1 Non-dimensionalization of the rotor equation

In order to put the rotor equation (3) into non-dimensional form a number of additional variables are introduced:

$$\mu = \frac{m}{M}, \quad \zeta = \frac{C}{\sqrt{MK}}, \quad F_{x*} = \frac{F_x}{h_0K}, \quad F_{y*} = \frac{F_y}{h_0K}, \quad \sigma = \frac{s}{R}, \tag{40}$$
$$\omega_0^2 = \frac{K_x}{M}, \quad \chi = \frac{K_y}{K_x}.$$

Applying these to (3) under the assumption that the rotor undergoes steady whirl with frequency $\tilde{\omega}_0$, we obtain

$$\begin{aligned} &\epsilon^2\left[-\tilde{\omega}_0^2\begin{bmatrix}1+\mu & 0\\ 0 & 1+\mu\end{bmatrix} + \mathrm{i}\tilde{\omega}_0\begin{bmatrix}\zeta\bar{\omega}_0 & -2(1+\mu)\\ 2(1+\mu) & \zeta\bar{\omega}_0\end{bmatrix}\right. \\ &\left. + \begin{bmatrix}\bar{\omega}_0^2 - (1+\mu)\Omega_*^2 & -\zeta\Omega_*\\ \zeta\Omega_* & \chi\bar{\omega}_0^2 - (1+\mu)\end{bmatrix}\right]\begin{Bmatrix}x_*\\ y_*\end{Bmatrix} \\ &= \epsilon^2\begin{Bmatrix}\mu\sigma\delta^{-\frac{1}{2}}\\ 0\end{Bmatrix} + \epsilon\begin{Bmatrix}F_{x*}\\ F_{y*}\end{Bmatrix}, \end{aligned} \tag{41}$$

where $\bar{\omega}_0 = \omega_0/\Omega$.

4.2 Fluid forces

The fluid force components F_x and F_y on the right hand side of (3) can be split up into pressure- and friction-related parts, indicated by subscripts p and f respectively, as follows:

$$\frac{F_{xp}}{RL} = \int_0^{2\pi} p(0)\cos\xi d\xi, \quad \frac{F_{yp}}{RL} = \int_0^{2\pi} p(0)\sin\xi d\xi, \tag{42}$$

$$\frac{F_{xf}}{RL} = \int_0^{2\pi} \rho\eta U^2\sin\xi d\xi, \quad \frac{F_{yf}}{RL} = -\int_0^{2\pi} \rho\eta U^2\cos\xi d\xi, \tag{43}$$

where L is the length (height) of the vessel. In the following only the pressure-related terms will be considered. The non-dimensional version of these terms - to be inserted into (41) - take the simple forms

$$F_{x*} = \int_0^{2\pi} p_*(\xi, 0) \cos\xi \, d\xi, \quad F_{y*} = \int_0^{2\pi} p_*(\xi, 0) \sin\xi \, d\xi. \tag{44}$$

5 Hydraulic jump solution

The first three terms on the left hand side of (37) represent a Korteweg-de Vries-type equation, while the first, second, and fourth term represent a Burgers-type equation. The homogeneous Korteweg-de Vries equation is known to have analytical solutions in forms of solitary and cnoidal waves, depending on the boundary conditions. Analytical solutions to homogeneous and non-homogeneous Burgers equations are also known [9, 10]. On the other hand, analytical solutions to non-homogeneous Korteweg-de Vries equations are known only for a few special cases, e.g. [11]. In whatever way, the forced Korteweg-de Vries-Burgers equation (37) is expected to have a variety of interesting solutions.

We seek a solution which can 'extinguish' the forcing effect of the unbalance mass and it is instructive to obtain a simple, analytical solution, even if one has to 'oversimplify' the basic equations, that is, to make assumptions that are not fully physical sound. The solution obtained in this way should then be assessed by comparison with analytical or numerical solutions of the (physically sound) basic equations.

Such a solution of (37) can be obtained if one assumes:

- no dispersion $\Rightarrow \partial^3\kappa_0/\partial\xi^3 = 0$;
- no friction $\Rightarrow \nu_* = \eta_* = 0$.

Then it reduces to

$$A_1 \frac{\partial\kappa_0}{\partial\xi} - B_1\kappa_0 \frac{\partial\kappa_0}{\partial\xi} = x_* \sin\xi - y_* \cos\xi, \tag{45}$$

Integration gives

$$A_1\kappa_0 - \frac{1}{2}B_1\kappa_0^2 = -x_* \cos\xi - y_* \sin\xi + \mathcal{A}, \tag{46}$$

where $\mathcal{A}$ is an integration constant. Solving (46) with respect to κ_0 gives

$$\kappa_0(\xi) = \frac{A_1}{B_1} \pm \left\{ \left(\frac{A_1}{B_1}\right)^2 + \frac{2}{B_1}\left(x_* \cos\xi + y_* \sin\xi - \mathcal{A}\right) \right\}^{\frac{1}{2}}. \tag{47}$$

The change of sign ($\pm$) in (47) gives a discontinuity which represents a hydraulic jump, as illustrated in Fig. 3. Let the jump be located at $\xi = \Upsilon$, $0 < \Upsilon < 2\pi$, in terms of the rotating polar coordinate system discussed in the beginning of Section 3. Assuming that it is not located at $\xi = 0$ or 2π (i.e. at the same location as the unbalance mass) gives the following 'smoothness condition' at this point:

$$\kappa_0(0) = \kappa_0(2\pi). \tag{48}$$

The constant $\mathcal{A}$ can be determined from this condition, which gives

$$\mathcal{A} = \frac{B_1}{2}\left(\frac{A_1}{B_1}\right)^2 + x_*. \tag{49}$$

The solution of (45) is then given by

$$\kappa_0(\xi) = \kappa_\pm(\xi) = \frac{A_1}{B_1} \pm \left(\frac{2}{B_1}\right)^{\frac{1}{2}} \left\{x_*\left(\cos\xi - 1\right) + y_* \sin\xi\right\}^{\frac{1}{2}}. \tag{50}$$

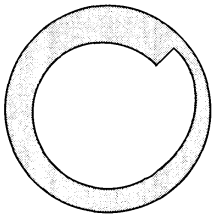

Figure 3: Sketch of the hydraulic jump solution, eqn. (50).

Let $p_{\pm}(\xi,0)$ be the fluid pressure corresponding to the depth perturbation $\kappa_{\pm}(\xi)$. The fluid forces are then given by

$$\begin{aligned} F_{x*} &= \int_0^{2\pi} p_*(\xi,0)\cos\xi\, d\xi \\ &= \int_0^{\Upsilon} p_-(\xi,0)\cos\xi\, d\xi + \int_{\Upsilon}^{2\pi} p_+(\xi,0)\cos\xi\, d\xi, \\ F_{y*} &= \int_0^{2\pi} p_*(\xi,0)\sin\xi\, d\xi \\ &= \int_0^{\Upsilon} p_-(\xi,0)\sin\xi\, d\xi + \int_{\Upsilon}^{2\pi} p_+(\xi,0)\sin\xi\, d\xi. \end{aligned} \tag{51}$$

The condition for mass conservation can be expressed as

$$\int_0^{2\pi} \kappa_0(\xi)\, d\xi = 0 \;\Rightarrow\; \int_0^{\Upsilon} \kappa_-(\xi)\, d\xi + \int_{\Upsilon}^{2\pi} \kappa_+(\xi)\, d\xi = 0. \tag{52}$$

The integrals in (51) and (52) are of elliptic types and cannot be evaluated in closed form. In order to obtain simple closed-form expressions we seek to approximate the square root in (50). As both terms under the square root are of the same order of magnitude a Taylor expansion does not exist.

But by assuming that $x_*, y_* \ll 1$, Lanczos's tau method [12] can be used. Logarithmic differentiation of the function $f(x) = \sqrt{x}$ gives the differential equation $f'(x) - \frac{1}{2}\frac{1}{x}f(x) = 0$. The initial condition $f(0) = 0$ assures the solution $f(x) = \sqrt{x}$. The tau method however approximates the solution via expansion in Chebyshev polynomials. Retaining only the linear part of this expansion, we obtain

$$\sqrt{x} \approx \frac{1}{3}(1+2x). \tag{53}$$

Equation (50) can thus be approximated as

$$\kappa_0(\xi) = \kappa_{\pm}(\xi) = \frac{A_1}{B_1} \pm \frac{1}{3}\left(\frac{2}{B_1}\right)^{\frac{1}{2}} \{1 + 2x_*(\cos\xi - 1) + 2y_*\sin\xi\}. \tag{54}$$

Using this expression the integrals in (51) and (52) can be evaluated in closed form. Doing this we obtain the coupled fluid-structure equation system

$$\begin{aligned} &\left[-\tilde{\omega}_0^2 \begin{bmatrix} 1+\mu & 0 \\ 0 & 1+\mu \end{bmatrix} + \mathrm{i}\tilde{\omega}_0 \begin{bmatrix} \zeta\bar{\omega}_0 & -2(1+\mu) \\ 2(1+\mu) & \zeta\bar{\omega}_0 \end{bmatrix} \right. \\ &\left. + \begin{bmatrix} \bar{\omega}_0^2 - (1+\mu)\Omega_*^2 & -\zeta\Omega_* \\ \zeta\Omega_* & \chi\bar{\omega}_0^2 - (1+\mu) \end{bmatrix} + \begin{bmatrix} \mathfrak{F}_{xx} & \mathfrak{F}_{xy} \\ \mathfrak{F}_{yx} & \mathfrak{F}_{yy} \end{bmatrix} \right] \begin{Bmatrix} x_* \\ y_* \end{Bmatrix} \\ &= \begin{Bmatrix} \mu\sigma\delta^{-\frac{1}{2}} \\ 0 \end{Bmatrix} + \begin{Bmatrix} \mathcal{F}_{rx} \\ \mathcal{F}_{ry} \end{Bmatrix}, \end{aligned} \tag{55}$$

where $\mathfrak{F}_{xx}, \ldots, \mathcal{F}_{rx}, \ldots$ are functions of the jump location Υ, given by

$$\begin{aligned}
\mathfrak{F}_{xx} &= -2\mathcal{K}_1\{\mathcal{P}_0(-\cos\Upsilon\sin\Upsilon + 2\sin\Upsilon - \Upsilon + \pi) + \mathcal{P}_1(\cos\Upsilon\sin\Upsilon + \Upsilon - \pi)\}, \\
\mathfrak{F}_{xy} &= -2\mathcal{K}_1(\mathcal{P}_0 - \mathcal{P}_1)(\cos^2\Upsilon - 1), \\
\mathfrak{F}_{yx} &= -2\mathcal{K}_1\{\mathcal{P}_0(\cos^2\Upsilon - 2\cos\Upsilon + 1) + \mathcal{P}_1(1 - 2\cos^2\Upsilon)\}, \\
\mathfrak{F}_{yy} &= -2\mathcal{K}_1(\mathcal{P}_0 - \mathcal{P}_1)(\cos\Upsilon\sin\Upsilon + \Upsilon - \pi), \\
\mathcal{F}_{rx} &= -2\mathcal{K}_1\mathcal{P}_0\sin\Upsilon, \\
\mathcal{F}_{ry} &= -2\mathcal{K}_1\mathcal{P}_0(1 - \cos\Upsilon).
\end{aligned} \tag{56}$$

Herein

$$\begin{aligned}
\mathcal{P}_0 &= 2\left(1 + 2\delta^{\frac{1}{2}}\frac{c_-}{c_0}\right), \quad \mathcal{P}_1 = \delta^2\left(\frac{c_-}{c_0}\right)^2, \\
\mathcal{K}_0 &= \frac{A_1}{B_1}, \qquad \mathcal{K}_1 = \pm\frac{1}{3}\left(\frac{2}{B_1}\right)^{\frac{1}{2}}.
\end{aligned} \tag{57}$$

The mass conservation equation (52) takes the form

$$2\mathcal{K}_1\{(\Upsilon - \sin\Upsilon - \pi)x_* + (\cos\Upsilon - 1)y_*\} + \mathcal{K}_0\pi + \mathcal{K}_1(\pi - \Upsilon) = 0. \tag{58}$$

For a given angular velocity Ω_*, (55) and (58) contain three equations for the three unknowns x_*, y_*, and Υ, which can be solved together numerically. [Here, $\mathcal{K}_0$ is set equal to zero in (58).] In the numerical example to follow we set $\delta = 0.125$, $\mu = 0.25$, $\zeta = 13.0$, $\sigma = 0.4$, and $\chi = 1.0$. In Fig. 4, part (a) shows the rotor amplitudes x_* and y_*, while part (b) shows the jump location (with Υ in radians). It is noted that the value of the damping parameter ζ is large, which implies the 'smooth' form of the x_* and y_* curves.

Part (b) shows that the jump is located at $\Upsilon \approx \pi$ for small values of the angular velocity Ω_* and that Υ increases smoothly with increasing value of Ω_*, up to $\Upsilon \approx 4.6$ rad. This is not the way the fluid balancer is expected to work (see Section 1). The results appear to indicate, then, that mechanism of the fluid balancer must be one or more solitary waves (solitons). This remains to be verified.

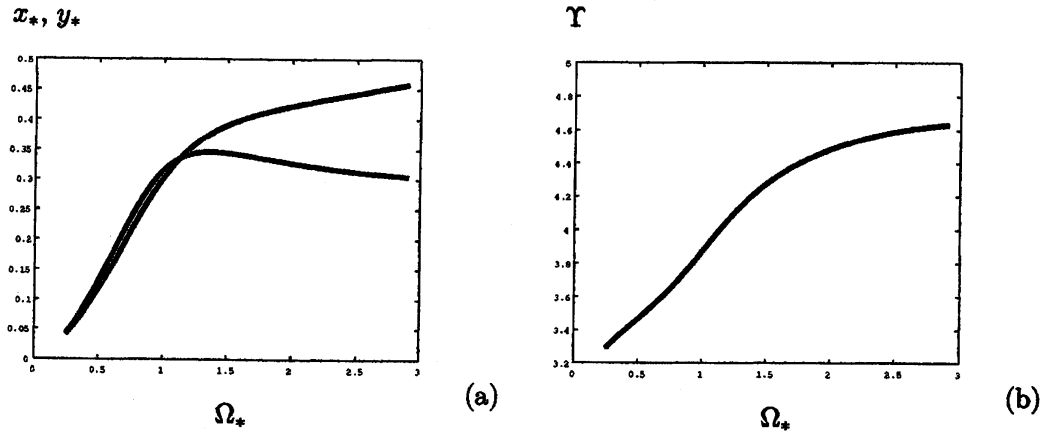

Figure 4: (a) Deflections x_* and y_* Lower curve: x_*; upper curve: y_*. (b) Jump location Υ.

6 Concluding remarks

The fluid balancer has been modeled as a rotor partially filled with fluid. The rotor has two degrees of freedom, and the fluid forces acting on it are evaluated in terms of shallow water theory.

A simplified analysis, giving a solution resembling a hydraulic jump, has been discussed in detail. It appears that this solution cannot represent the mechanism of the fluid balancer. Future work should thus consider soliton-type solutions of the Korteweg-de Vries-Burgers equation (37).

References

[1] Nakamura, T., 2009. "Study on the improvement of the fluid balancer of washing machines". In Proceedings of the 13th Asia-Pacific Vibrations Conference, 22-25 November 2009, University of Canterbury, New Zealand, pp. 1–8.

[2] Bolotin, V. V., 1963. *Nonconservative Problems of the Theory of Elastic Stability.* Pergamon Press, Oxford.

[3] Crandall, S. H., 1995. "Rotor dynamics". In Nonlinear Dynamics and Stochastic Mechanics, W. Kliemann and N. S. Namachivaya, eds., CRC Press, Boca Raton, pp. 1–44.

[4] Berman, A. S., Lundgren, T. S., and Cheng, A., 1985. "Asyncronous whirl in a rotating cylinder partially filled with liquid". *J. Fluid Mech.,* ***150***, pp. 311–327.

[5] Colding-Jorgensen, J., 1991. "Limit cycle vibration analysis of a long rotating cylinder partly filled with fluid". *J. of Eng. for Gas Turbines and Power,* ***113***, pp. 563–567.

[6] Kasahara, M., Kaneko, S., and Ishii, H., 2000. "Sloshing analysis of a whirling ring". In Proceedings of the Dynamics and Design Conference 2000, 5-8 August 2000, Japan Soc. Mech. Eng., pp. 1–6.

[7] Yoshizumi, F., 2007. "Self-excited vibration analysis of a rotating cylinder partiall filled with liquid (Nonlinear analysis by shallow water theory)". *Trans. Japan Society of Mech. Eng. (C),* ***73***(735), pp. 28–37.

[8] Green, K., Champneys, A. R., and Lieven, N. J., 2006. "Bifurcation analysis of an automatic dynamic balancing mechanism for eccentric rotors". *J. Sound Vib.,* ***291***, pp. 861–881.

[9] Whitham, G. B., 1999. *Linear and Nonlinear Waves.* Wiley-Interscience, New York, NY.

[10] Petrovshii, S. V., 1999. "Exact solutions of the forced Burgers equation". *Tech. Phys.,* ***44***(8), pp. 878–881.

[11] Smyth, N. F., 1987. "Modulation theory solution for resonant flow over topography". *Proc. R. Soc. Lond. A,* ***409***, pp. 79–97.

[12] Lanczos, C., 1956. *Applied Analysis.* Prentice-Hall.